Big root approximation of site-scale vegtation water uptake

Martin Bouda[1]

[1]Faculty of Forestry and Wood Sciences, Czech University of Life Sciences in Prague, Kamýcká 129, 165 21, Prague, Czech Republic

22.2.2019

Abstract

Land surface model (LSM) predictions of soil moisture and transpiration under water-limited conditions suffer from biases due to a lack of mechanistic process description of vegetation water uptake. Here, I derive a 'big root' approach from the porous pipe equation for root water uptake and compare its predictions of soil moistures during the 2010 summer drought at the Wind River Crane site to two previously used Ohm's law analogue plant hydraulic models. Structural error due to inadequate representation of root system architecture (RSA) in both Ohm's law analogue models yields significant and predictable moisture biases. The big root model greatly reduces these as it better represents RSA effects on pressure gradients and flows within the roots. It represents a major theoretical advance in understanding vegetation water limitation at site scale with potential to improve LSM predictions of soil moisture, temperature and surface heat, water, and carbon fluxes.

Introduction

As vegetation takes up carbon dioxide to fix the sun's energy, it loses water vapour to the surrounding atmosphere and draws liquid water from the soil to prevent leaf dessication. Globally, this process of transpiration returns almost 40% of water fallen over land to the atmosphere [1]. Transpiration also cools the land surface, as the water phase change binds heat to the vapour, and the attendant latent heat flux represents about a third of the heat received by the land surface as a result of its net radiation balance [2]. Transpiration is also strongly coupled to the surface carbon flux, as the leaf exchanges one molecule of carbon dioxide for about 400 molecules of water [3]. When vegetation is water-limited, it must reduce its rate of carbon assimilation or face dessication, reducing primary productivity [4]. Despite the key role that vegetation access to soil water can play in limiting terrestrial fluxes of water, heat and carbon dioxide, it remains poorly understood at relevant scales.

A lack of accurate descriptions of plant water limitation gives rise to significant prediction errors in terrestrial or land surface models (LSM), which aim to predict these surface fluxes as a bottom boundary condition on atmospheric circulation in earth system simulations [5, 6, 7]. A common approach in large-scale land surface, dynamic vegetation or ecosystem dynamics models is to calculate water uptake from each soil layer in proportion to an assumed root length density fraction reduced by a stress factor, which is often a linear function of local soil moisture status [8, 9, 10, 11, 12, 13, 14, 7, 15, 16, 17, 18]. It has been shown that changing this root water uptake formulation can give rise to significant differences in predicted transpiration across models [19, 20]. Results from Coupled Model Intercomparison Project Phase 5 (CMIP5) simulations of the Intergovernmental Panel on Climate Change (IPCC) show overestimates of evapotranspiration and associated overland cooling in most terrestrial regions, especially under soil-moisture limited ET regimes [21]. CMIP5 simulations undeline the critical role of plant access to variable soil moisture in mediating surface-atmosphere fluxes and vegetation dynamics [22]. As awareness of the importance of plant hydraulics for ecosystem ecology and earth system science has grown [23], it has become apparent that it is desirable to make LSM descriptions of plant hydraulics more mechanistic to better capture vegetation behaviour during drought [24], especially since the frequency of such water-limiting events is likely to increase in the future [25].

This has given an impetus to replace the classical plant water stress formulation with a more process-based model [26, 27, 28], based on an Ohm's law analogue for water flow in plants [29]. While such an approach works well for stems, its weakness in representing root water uptake is that it places all plant resistances between the root base and each soil layer either exclusively in parallel [29] or in series [30]. Each of these configurations is an end-member of the spectrum of possible root system architectures (RSA) in that all other RSAs combine resistances to within-plant flow between layers in series with resistances in parallel. The actual arrangment of resistances in RSA is crucial to controlling uptake from variably saturated soils [31, 32, 33, 34, 35], as it determines the rate at which water uptake dissipates water potential gradients [36, 37], which drive flow along the soil-plant-atmosphere continuum [29]. As water uptake in a given layer dissipates the potential gradient between adjacent layers, it reduces how much water can be taken up in deeper layers. The strength of this effect depends on the soil water potentials in adjacent layers and the full arrangement of resistances. Whereas the

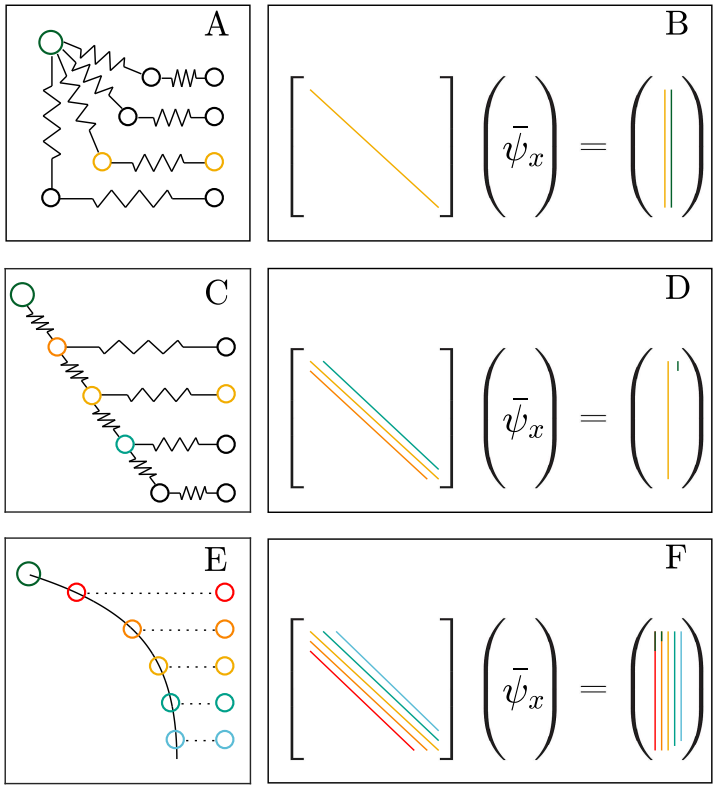

Figure 1: Comparison of conceptual models: Resistance diagrams for the Ohm's law models with subsequent soil layers connected to the root base in parallel (A) and in series (C). Conceptual diagram of big root model (E) as a discretised form of the solution to the continuous porous pipe equation. Circles represent water potentials at the root base (green, top left), in the soil (right-most column) and within the root (inner nodes in resistance networks in A and C, and along the solid root water potential curve in E). Sparsity patterns and composition of linear systems for layer root water potential ($\bar{\psi}_x$) in the Ohm's law parallel (B), series (D), and big root (F) models, colour-coded to correspond to elements in conceptual diagrams. Coefficient matrices show non-zero diagonals present in each model, with gold on the main diagonal (layer being solved for), orange and red for layers above and dark and pale blue for layers below. Right hand side vector entries are linear combinations of the soil water potentials of individual layers, identically colour coded. Green denotes a term for the root base boundary condition. Coloured nodes in conceptual diagrams show elements involved in the solution for root water potential in gold layer.

parallel resistance structure (Fig. 1A) only allows uptake in one layer to affect others via the potential at the root base, the model that places all layers in series (Fig. 1C) assumes that the plant water potential value effective in uptake and in transport are the same in a given layer, oversimplifying the effects of adjacent water potential values on each other. Neither is a suitable conceptual model for the complex cross-layer effects known to emerge in spatially explicit RSA simulations [36].

A conceptual alternative is provided by the 'porous pipe' model of root water uptake [38], which describes the continuous variation of water potential (ψ) along the length (s) of roots taking up water with the differential equation

$$\frac{d^2\psi_x}{ds^2} = \frac{k_r}{K_x}(\psi_x - \psi_s)\,, \tag{1}$$

where the left-hand side term represents the dissipation of the gradient of root water potential (ψ_x), which is proportional to the water potential difference between the root and the soil (ψ_s), with the ratio of conductance into (k_r) and along (K_x) the root as the constant of proportionality. Analytical solutions to this equation have recently been extended from the case of single roots with homogeneous properties to arbitrary RSAs [39, 37]. This paves the way for solutions to this continuous model that predict the root water potential effective in water uptake in each layer ($\bar{\psi}_x$) as a function of varying soil water potentials and canopy demand (Fig. 1E). Here, I show that analytical solutions for $\bar{\psi}_x$ can be obtained from a linear system of equations for different RSAs and constraining the linear coefficients as for a single root (a 'big root' model) yields improved predictions of vegetation water uptake during a drought at a forested site, as compared to the Ohm's law models.

Results

Model Form

For a single root traversing soil layers of uniform water potential, the water potential effective in water uptake in the ith layer can be expressed as

$$\bar{\psi}_x^i = \sum_{j=i-2}^{i+2} \xi^j \bar{\psi}_x^j + \sum_{k=i-2}^{i+2} \sigma^k \psi_s^k,\ (j \neq i), \tag{2}$$

with linear coefficients ξ and σ derived analytically from root properties (see Methods). A root system with a single junction and two daughter branches of unequal properties that each cross into further soil layers can be described by an equation of the same form but with an intercept (see SI Analysis). Given field data on the uptake of root systems of unknown RSA, it is impossible to construct the coefficients analytically. As constraints are needed to find useful values by model inversion (SI Computations), using the expressions for linear coefficients fromn the single-root case as constraints on the model inversion to field data, a 'big root' approach, is the simplest method of arriving at site-scale model parameters.

Both the Ohm's law models and the big root model (eq. 2) can be formulated as linear systems, whose solution is the vector of root water potential values for each layer. The models differ in the sparsity pattern of their coefficient matricies and the composition of the terms in the right-hand side vector. In the layers-in-parallel Ohm's law model, each layer's root water potential value depends only on the same layer's soil water potential and the root base boundary condition (Fig. 1B). In the layers-in-series model it depends instead on the root water potentials in the layers above and below, as well as the same

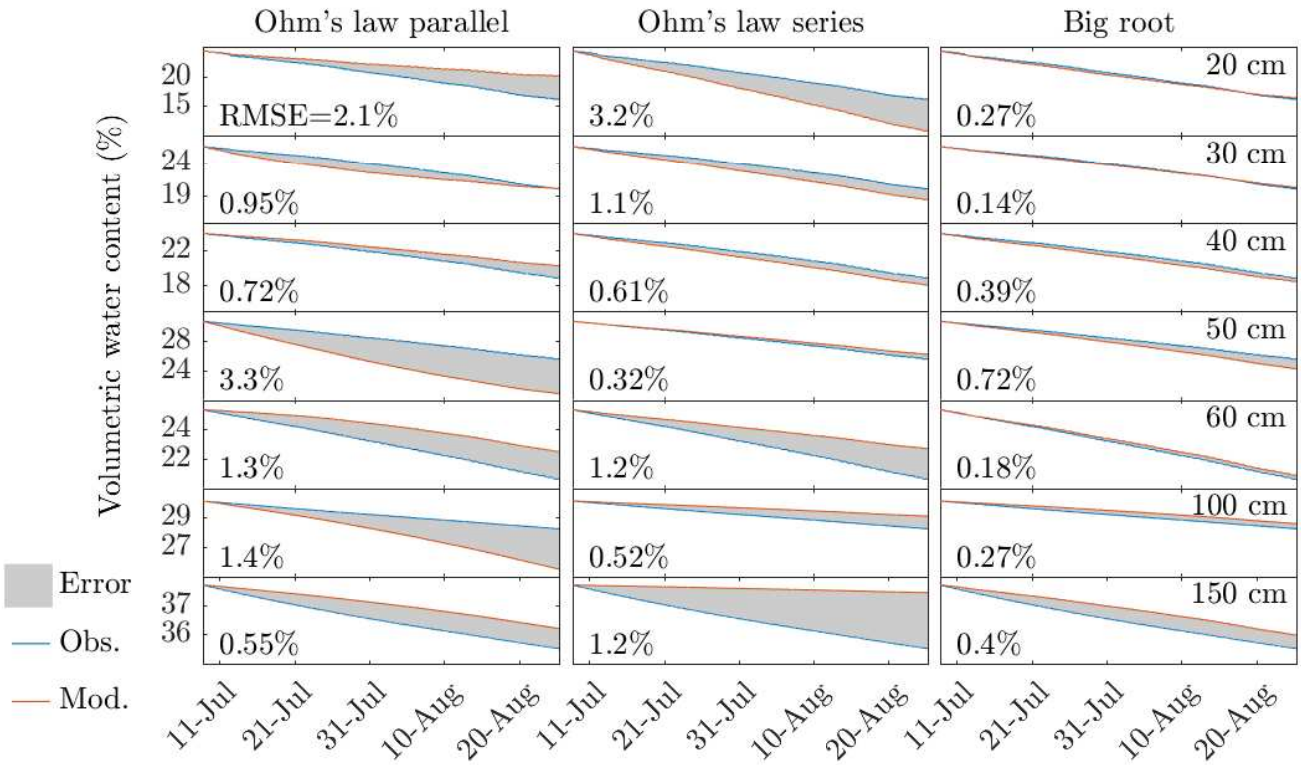

Figure 2: Observed (blue) and predicted (red) volumetric soil moisture (%) over the entire simulation period for the Ohm's law parallel (left), series (centre), and big root (right) models, divided by soil layers (depths at right). Root Mean Square Error of prediction reported at left of each panel.

layer's soil water potential; only in the top layer is the root base boundary condition relevant (Fig. 1D). In the big root model, by contrast, the root water potential in a given layer depends on the root and soil water potentials of two layers above and the two below; only in the two topmost layers is the root base boundary condition relevant (Fig. 1F). The big root model thus represents more complex interactions between depth layers without noticeably increasing the computational cost of the calculation.

Numerical Simulations

Each model was used to predict the course of vegetation water uptake and soil moisture during the 2010 summer drought at the Wind River Crane site [40, 41, 42]. The layers-in-parallel Ohm's law model had the highest overall root mean squared error (RMSE) in soil moisture predictions (10.32% summed across layers), with both significant dry and wet biases in different layers (Fig. 2, left). A major source of error in this model was spurious soil moisture redistribution. In the shallow soil layer, this led to increasing nocturnal water outflow over time, even as the model predicted nocturnal excessive uptake at 50 and 100cm depths (Fig. 3a-b,g,k-l). This redistribution so depletes the 50cm layer over the first half of the simulation (Fig. 3g) that it is unable to to support observed root water uptake later on (Fig. 3h), furhter increasing spurious uptake at 100cm (Fig. 3l). The parallel model accumulates least bias at a depth of 30cm by the end of the simulation, but this is because its initial overprediction of peak uptake rates (Fig. 3c) is compensated in the second half of the simulation by spurious nocturnal water redistribution into the layer (Fig. 3D). As root water inflow or outflow in a given layer is linear in the difference between stem base and soil water potential in this model, water flows freely across layers via the stem base. The assumed RSA thus leads to excessive smoothing of the soil moisture profile over time, with wet biases in dry soil layers and dry biases in wetter layers.

The layers-in-series model performs slightly better for these data overall (8.15% RMSE across all layers) but had persistent errors of consistent structure. The model consistently yields dry biases in shallow soil layers and wet biases in deep layers (Fig 2, centre), which are apparent at the half-hourly scale, for all times and throughout the simulation period (Fig. 3). This persistent error structure follows from the assumed RSA, as the water potential gradient is constrained to vary too rigidly with depth. The serial arrangement of resistamces subjects shallow roots to overly negative water potentials leading to uptake overestimates but sustains only slightly negative potentials at depth, leading to underestimated uptake.

The big root model performed best out of the three at predicting the time-course of soil moisture (2.37% RMSE overall, Fig. 2, right). It did have trouble simulating nocturnal outflows at 50cm (Fig. 3g,h), leading to a slight dry bias at this depth over time. This was matched by a slight wet bias in

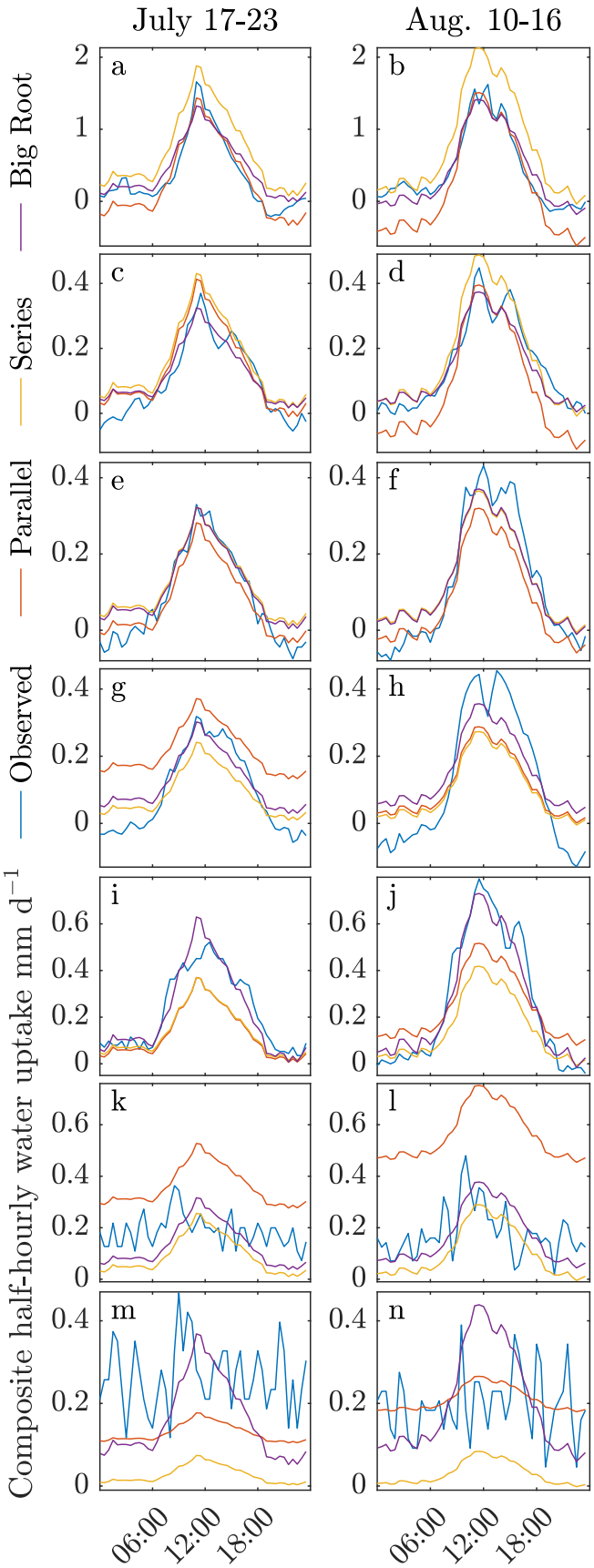

Figure 3: Comparison of observed and modelled half-hourly water uptake rate (mm/d) for 6-day composites of periods outside calibration dataset, displayed separately for each depth layer.

the two deepest layers (100 and 150cm), which may be the source of hydraulic redistribution to 50cm in the data. All three models had trouble with the dynamics of the two deepest layers, where observations did not exhibit diurnal cycling of moisture loss, likely breaching the calibration assumption that all water movement is through the vegetation. The big root model had lowest bias in these layers, showing that while it did not simulate the diurnal course of uptake well, it was best at predicting its mean level. In all layers except at 50cm, RMSE of soil predicted moistures was below 0.5%, in all other layers with a diurnal uptake signal model fit (Nash Sutcliffe Efficiency) was above 0.75, and in all layers the overall model bias was below 0.05 mm/d, outperforming the Ohm's law models (Fig. 4). The big root model better predicted the time-course of root water potential than either Ohm's law model because of its better representation of RSA, enabling it to significantly reduce biases in soil moisture predictions.

Discussion

The derivation of an analytical big root model of root water uptake is a major theoretical advance in the description of vegetation access to soil water. Both Ohm's law analogue models revealed their structural limits in representing the important effects of RSA on water potential gradients and thus water uptake. The resistances-in-parallel model overpredicted uptakes in wet layers and excessively redistributed water to dry layers, consistently with performance in LSMs [28]. The resistances-in-series model overestimated uptake in shallow layers and underestimated in at depth. Both error structures follow from the models' respective assumed RSA and the resulting water potential gradient configurations. The big root model, by contrast, was able to account for most of the complex effects of RSA on the dissipation of water potential gradients with uptake, leading to the virtual elimination of biases in the shallow layers. The reduced, but persistent biases in the deep layers may be an artefact of calibration assumptions in the present study, rather than a feature of the model itself. Accounting for the effects of RSA in water uptake is thus a step towards reducing important soil moisture, as well as transpiration and heat flux biases identified in CMIP5 simulations [21].

The form of the big root model, eq. 2, reveals it to be a special case of the RSA Stencil model that accurately predicts uptake by root systems of a variety of RSA [36]. Supplementary derivation shows that for more complicated RSA, the linear coefficients have more complex relations to the underlying root properties and that unequal properties in different root system branches within a single soil layer give rise to an intercept in the equation. This functional form is fully consistent with RSA Stencils previously fitted to the uptake of more complex root systems [36]. It may be conjectured on this basis that the coefficients and intercept of an RSA Stencil can be derived analytically for any RSA, subject to the assumptions of the porous pipe model and soil moisture homogeneity within layers.

Constraining the RSA Stencil to behave as a single root sacrifices flexibility in fitting data but imposes mechanistic

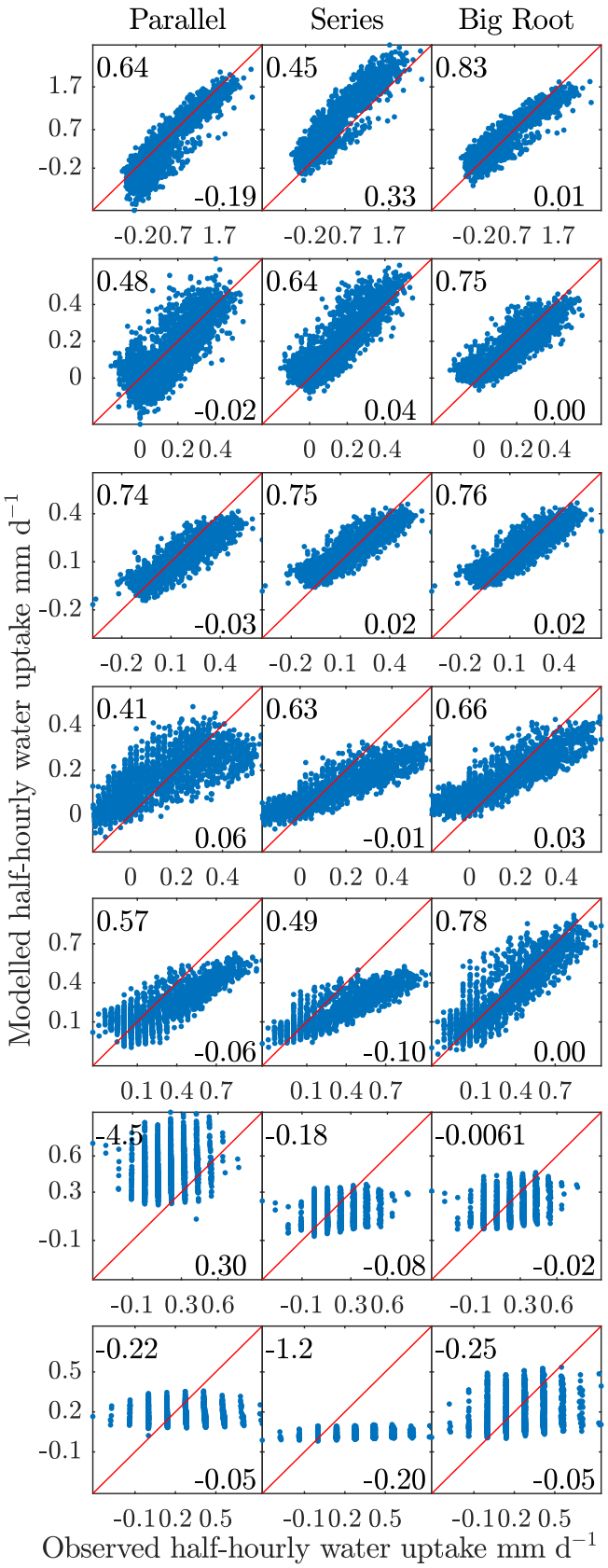

Figure 4: Model vs. observed half-hourly water uptake (mm/d) covering entire period, for each model (columns) and all dephts (rows); 1:1 line in red, Nash-Sutcliffe Efficiency at top left and model bias (mm/d) at bottom right.

consistency onto model predictions, when outside the range of calibration. If the major source of prediction error for the big root model in this dataset was its inability to predict hydraulic redistribution to the 50cm depth from below 100cm, this is presumably because a single root can simply not behave this way without sacrificing model fit elsewhere in the calibration dataset. Supplementary inversions (SI Computations) show that unconstrained RSA Stencils can easily be made to predict either uptake dynamics or soil moistures, though not both, likely because of over-fitting. While a better fit to both may in theory be possible, it would not be robust outside the calibration range. Instead, it is possible to construct a more robust predictive model by deriving the linear coefficient constraints for a sufficiently complex RSA that is capable of all important water uptake dynamics present in a dataset. The robustness of predictions, based on accurate representations of mechanisms, is especially important in the context of future climate projections, where vegetation water uptake potentially takes place in no-analogue scenarios.

To allow for borader application of a big root model in LSMs, its parameter values need to be established for a number of sites with distinct plant functional types (PFTs). The calibration procedure is data-intensive and subject to some restrictive assumptions. It is particularly important to arrive at an adequate partitioning of root water uptake from soil water movement prior to calibration. Model calibration is also sensitive to the soil moisture characteristic (θ-ψ_s) curve, as the model is linear in soil water potential, which is itself very nonlinear in soil moisture. Ideally, the calibration dataset would contain both sets of values, directly observed. Preliminary model inversions (SI Computations) suggest that it is possible to find meaningful root hydraulic parameters (total layer soil-root conductance and cross-layer root conductance) rather than just RSA Stencil linear coefficients useful in predicting uptake, as was done here. The necessary condition is to have data on xylem water potential at the base of the root system for each time-step, which can be obtained through stem psychrometry [43]. Obtaining time-series of how such effective 'big root' parameters change at different time scales in real vegetation may lead to insights concerning the importance of underlying biological mechanisms (e.g. root growth and senescence, aquaporin activity) at larger scales.

The main limitation of the big root model follows from the assumption that soil moisture is uniform in each layer. Lateral soil moisture heterogeneity is a key feature of unsaturated zone hydrology and neglecting it necessarily leads to model prediction error [33]. This assumption is not novel in the big root model, however, but is instead a feature of all LSMs. In fact, it was assumed at the outset of model development to ensure compatibility of the result with relevant LSMs and maintain sufficiently low computational cost. The model might, however, be extended to account for lateral soil moisture heterogeneity, for example by separately modelling a 'dry' and 'wet' soil column, with a two-root model simulating a split root situation. Micro-scale heterogeneity, between the rhizospehere and 'bulk soil' can also be the key limiting factor to soil-root flows [44]. While it was not represented in this study, this resistance

can be modelled separately, in series with the RSA model [45]. Also, it is notable that not representing this mechanism in the big root model seemingly did little to degrade the quality of its predictions for the Wind River Crane data.

A big root model for site-scale vegetation water uptake can be derived from first principles describing water movement through plant roots. This formalism provides a simple and mechanistically based framework to describe a key process limiting land surface exchanges of matter and energy. There are many potential applications of the theory beyond terrestrial modelling, principally in agronomy, where it may serve to improve on existing crop models, which often rely on empirical or heuristic formalisms to predict crop yields, and thus food production, in future climate scenarios. Further analytical work can extend the RSA Stencil framework to increase realism by deriving analytical constraints for two- or n-root models that improve model skill without increasing computational cost.

Methods

Model Development

Solutions to eq. 1 can be used to define a mean value of water potential effective in root uptake,

$$\bar{\psi}_x^i = \frac{\int_0^S \psi_x(s)ds}{S}\,, \tag{3}$$

for each segment of a root of known length S and with uniform axial (K_x) and radial (k_r) hydraulic conductances. This is the value of water potential that allows uptake of the root segment to be found as $Q_r = k_r S(\bar{\psi}_x - \psi_s)$. Solutions for this value,

$$\bar{\psi}_x^i = \psi_s^i + (G_1^i - G_0^i)/\beta_2^i \tag{4a}$$
$$\bar{\psi}_x^i = c_1^i\psi_0^i + (1-c_1^i)\psi_s^i - c_2^i G_0^i \tag{4b}$$
$$\bar{\psi}_x^i = c_3^i\psi_0^i + (1-c_3^i)\psi_s^i - c_4^i G_1^i \tag{4c}$$
$$\bar{\psi}_x^i = c_1^i\psi_1^i + (1-c_1^i)\psi_s^i + c_2^i G_1^i \tag{4d}$$
$$\bar{\psi}_x^i = c_3^i\psi_1^i + (1-c_3^i)\psi_s^i + c_4^i G_0^i \tag{4e}$$
$$\bar{\psi}_x^i = c_5^i(\psi_1^i + \psi_0^i) + (1-2c_5^i)\psi_s^i\,, \tag{4f}$$

are linear in the layer boundary conditions: soil water potential (ψ_s^i) and the root water potential (ψ^i) or its gradient (G^i) at layer boundaries (subscript 0 at layer bottom and 1 at top); linear coefficients c_j^i, $j \in 1,..,5$ are determined by root properties (k_r^i, K_x^i, S^i), as shown in table 1.

Assuming a single root segment traversing each soil layer, these linear relations for $\bar{\psi}_x$ of adjacent layers can be combined and the conditions at layer boundaries cancelled (Fig. 5) to yield eq. 2. The linear coefficients in these equations are known functions of the root segment properties k_r, K_x, and S (details of the derivation and resulting coefficient expressions in SI Analysis).

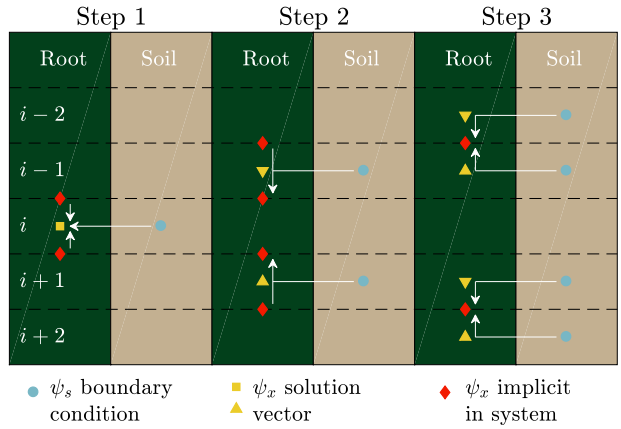

Figure 5: Assembly of big root linear equation for layer i. Step 1 selects an equation for $\bar{\psi}_x^i$ in boundary conditions at the top and bottom of the layer. Step 2 substitutes expressions for boundary conditions in layer i in boundary conditions at layers $i \pm 1$. Step 3 replaces boundary conditions at layers $i \pm 1$ with expressions in mean root and soil water potentials in layers $i \pm 1$ and $i \pm 2$. The result is an equation for mean root water potential in a given layer in terms of those in the four surrounding layers and the corresponding soil water potentials.

Given a boundary condition on water potential or its gradient at the stem base, a linear system constructed from eq. 2 may be solved simultaneously for the $\bar{\psi}_x$ in all soil layers, also yielding the uptakes Q_r. For a root of unknown properties on each segment, the model parameters k_r, K_x, and S can be estimated by inversion. By using the analytical relations between these parameters and the linear coefficients in eq. 2 as constraints when fitting the latter for unknown RSA, one calibrates a 'big root' model, which assumes that this RSA can effectively be represented as a single root.

Site and Data

Wind River crane precipitation and soil moisture data at half-hourly resolution for the year 2010 [42] were used in conjunction with published root length profiles (Fig. 6a) and soil characteristic curve (Brooks-Corey) parameters [46, 41]. The summer drought period was subselected from the data (Fig. 6b) as the period with no precipitation events that noticeably affect shallow-layer soil moisture. This was done in order to minimise soil water movement in the resulting dataset. Under the simplest assumption that all water movement during this period is due to plant water uptake or loss, root water uptake at each time-step was calculated from volumetric water content using centred differences. A calibration dataset of three 72-hour periods was further subselected from the drought period, at its start, middle, and end (Fig. 6c).

Numerical Simulations

All model inversions were performed using the assumption that all water movement in the dataset represents root water uptake or loss. Soil moisture was taken to be uniform in each

Table 1: List of variables

Symbol	Unit	Expression	Description	Role
$\bar{\psi}_x^i$	Pa	–	Mean xylem water potential in layer i	Dependent variable
ψ_s^i	Pa	–	Soil water potential in layer i	Boundary condition
ψ_0^i, ψ_1^i	Pa	–	Xylem water potential at bottom and top of layer i	Boundary condition
G_0^i, G_1^i	$\mathrm{Pa\,m^{-1}}$	–	Xylem water potential gradient at the bottom and top of layer i	Boundary condition
k_r^i	$\mathrm{m^2\,s^{-1}\,Pa^{-1}}$	–	R oot radial conductance per unit length in layer i	Model parameter
K_x^i	$\mathrm{m^4\,s^{-1}\,Pa^{-1}}$	–	Root axial conductance per unit length in layer i	Model parameter
S^i	m	–	Root length in layer i	Model parameter
α^i	$\mathrm{m^{-1}}$	$\sqrt{k_r^i/K_x^i}$	Square root of the ratio of radial to axial conductances per unit length	Derived parameter
β^i	1	$\alpha^i S^i$	Square root of the ratio of total layer radial conductance to total layer axial conductance	Derived parameter
β_2^i	$\mathrm{m^{-1}}$	$(\alpha^i)^2 S^i$	Ratio of radial to axial conductances per unit length times total layer length	Derived parameter
c_1^i	1	$\sinh(\beta^i)/\beta^i$	–	Linear Coefficient
c_2^i	1	$(1-\cosh(\beta^i))/\beta_2^i$	–	Linear Coefficient
c_3^i	1	$\tanh(\beta^i)/\beta^i$	–	Linear Coefficient
c_4^i	1	$(\mathrm{sech}(\beta^i)-1)/\beta_2^i$	–	Linear Coefficient
c_5^i	1	$\tanh(\beta^i/2)/\beta^i$	–	Linear Coefficient

layer. Calibration data included soil water potentials and calculated root water uptakes in each layer, as well as a flow boundary condition, found as the sum of water losses across all layers. The time-course of volumetric water content was not included in calibration data. The big root model was calibrated on the subset of three 72-hour periods. The inversion procedure estimated model parameters K_x, k_r, and S in each layer, although the absolute parameter values themselves are meaningless given the boundary conditions used, and served only to yield correctly constrained linear coefficients for eq. 2, capable of predicting root water uptakes (see SI Computations for details). Root conductances between layers in the Ohm's law in-series model was calibrated by inversion to the whole drought period, as parameters of satisfactory quality could not be found with the calibration subset alone. All inversions were performed using the Levenberg-Marquardt algorithm [47, 48]. Conductances from the stem base to each soil layer in the Ohm's law parallel model, as well as soil-root conductances in the in-series model, were set in proportion to the observed rooting profile.

Forward simulations with each model used soil moisture in each layer at the start of the drought period as the initial condition and solved for soil water contents at each subsequent time-step, with wtaer potentials calculated from predicted soil moistures. The simulation employed a Crank-Nicolson time-stepping scheme and represented the θ and ψ_s relationship implicitly, using an iterative solver to account for its nonlinearity [49, 50].

All computational work was done in Matlab, release R2018a [51]; all original code is available on request from the author.

Acknowledgments

I am deeply grateful to Sonia Wharton and the team at Wind River Crane who collected and kindly provided the data underlying the test case. This work was supported by The Ministry of Education, Youth and Sports (Czech Republic) through the institutional project MŠMT CZ.02.1.01/0.0/0.0/16 019/0000803 and the infrastructure project "IT4Innovations National Supercomputing Center LM2015070".

References

[1] Schlesinger, W. H. & Jasechko, S. Transpiration in the global water cycle. *AGRICULTURAL AND FOREST METEOROLOGY* **189**, 115–117 (2014).

[2] Wild, M. *et al.* The energy balance over land and oceans: an assessment based on direct observations and cmip5

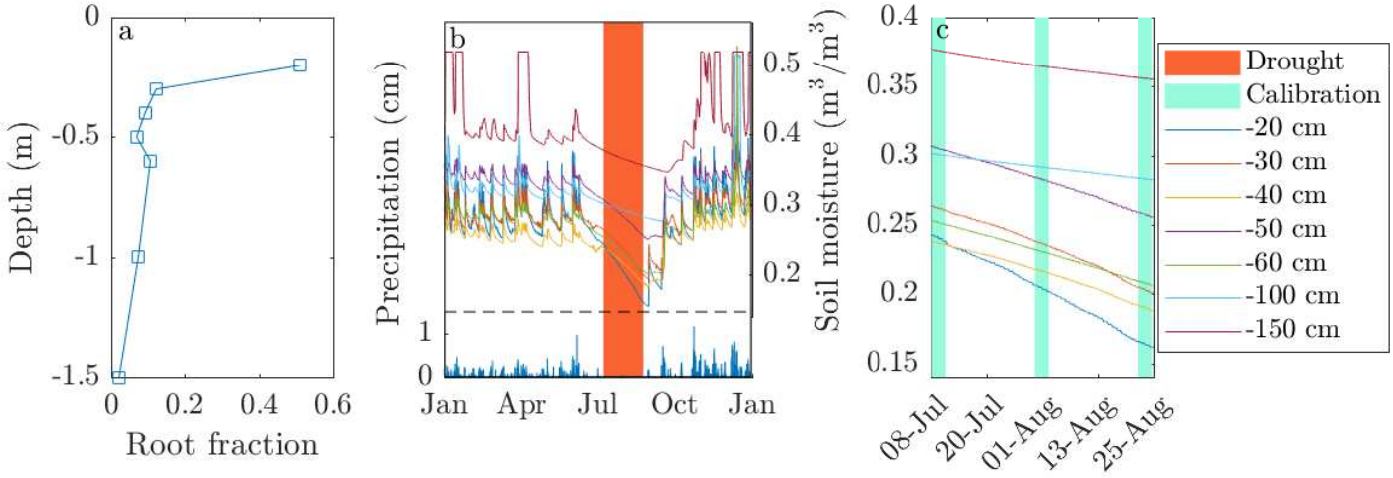

Figure 6: Wind River Crane data used: root profile (a) precipitation and soil moistures with drought period selected for simulation marked in orange (b). Detail of soil moisture at 7 depths during the selected drought period (c), with calibration data subset marked in cyan.

climate models. *CLIMATE DYNAMICS* **44**, 3393–3429 (2015).

[3] Nobel, P. S. *Physicochemical and Environmental Plant Physiology* (Elsevier, Amsterdam, 2009), 4th edn.

[4] Fatichi, S., Pappas, C. & Ivanov, V. Y. Modeling plant-water interactions: an ecohydrological overview from the cell to the global scale. *WILEY INTERDISCIPLINARY REVIEWS-WATER* **3**, 327–368 (2016).

[5] Dietze, M. C. *et al.* Characterizing the performance of ecosystem models across time scales: A spectral analysis of the north american carbon program site-level synthesis. *JOURNAL OF GEOPHYSICAL RESEARCH-BIOGEOSCIENCES* **116** (2011).

[6] Dahlin, K. M., Fisher, R. A. & Lawrence, P. J. Environmental drivers of drought deciduous phenology in the community land model. *BIOGEOSCIENCES* **12**, 5061–5074 (2015).

[7] De Kauwe, M. G. *et al.* Do land surface models need to include differential plant species responses to drought? examining model predictions across a mesic-xeric gradient in europe. *BIOGEOSCIENCES* **12**, 7503–7518 (2015).

[8] McMurtrie, R., Rook, D. & Kelliher, F. Modeling the yield of pinus-radiata on a site limited by water and nitrogen. *FOREST ECOLOGY AND MANAGEMENT* **30**, 381–413 (1990). INTERNATIONAL SEMINAR ON MANAGEMENT OF WATER AND NUTRIENT RELATIONS TO INCREASE FOREST GROWTH, CANBERRA, AUSTRALIA, OCT 19-22, 1987.

[9] Feddes, R. *et al.* Modeling root water uptake in hydrological and climate models. *BULLETIN OF THE AMERICAN METEOROLOGICAL SOCIETY* **82**, 2797–2809 (2001).

[10] Krinner, G. *et al.* A dynamic global vegetation model for studies of the coupled atmosphere-biosphere system. *GLOBAL BIOGEOCHEMICAL CYCLES* **19** (2005).

[11] Medvigy, D., Wofsy, S. C., Munger, J. W., Hollinger, D. Y. & Moorcroft, P. R. Mechanistic scaling of ecosystem function and dynamics in space and time: Ecosystem demography model version 2. *JOURNAL OF GEOPHYSICAL RESEARCH-BIOGEOSCIENCES* **114** (2009).

[12] Best, M. J. *et al.* The joint uk land environment simulator (jules), model description - part 1: Energy and water fluxes. *GEOSCIENTIFIC MODEL DEVELOPMENT* **4**, 677–699 (2011).

[13] Le Moigne, P. *et al.* Surfex scientific documentation. Tech. Rep., Météo-France/CNRS (2012).

[14] Oleson, K. W. *et al.* Technical description of version 4.5 of the community land model (clm). Tech. Rep., Repository of the National Center for Atmospheric Research (2013).

[15] Fisher, R. A. *et al.* Taking off the training wheels: the properties of a dynamic vegetation model without climate envelopes, clm4.5(ed). *GEOSCIENTIFIC MODEL DEVELOPMENT* **8**, 3593–3619 (2015).

[16] Kala, J. *et al.* Implementation of an optimal stomatal conductance scheme in the australian community climate earth systems simulator (access1.3b). *GEOSCIENTIFIC MODEL DEVELOPMENT* **8**, 3877–3889 (2015).

[17] Hidy, D. *et al.* Terrestrial ecosystem process model biome-bgcmuso v4.0: summary of improvements and new modeling possibilities. *GEOSCIENTIFIC MODEL DEVELOPMENT* **9**, 4405–4437 (2016).

[18] Drewniak, B. A. Simulating dynamic roots in the energy exascale earth system land model. *Journal of Advances in Modeling Earth Systems* (2019).

[19] Jing, C.-Q., Li, L., Chen, X. & Luo, G.-P. Comparison of root water uptake functions to simulate surface energy fluxes within a deep-rooted desert shrub ecosystem. *HYDROLOGICAL PROCESSES* **28**, 5436–5449 (2014).

[20] Ferguson, I. M., Jefferson, J. L., Maxwell, R. M. & Kollet, S. J. Effects of root water uptake formulation on simulated water and energy budgets at local and basin scales. *ENVIRONMENTAL EARTH SCIENCES* **75** (2016).

[21] Mueller, B. & Seneviratne, S. I. Systematic land climate and evapotranspiration biases in cmip5 simulations. *GEOPHYSICAL RESEARCH LETTERS* **41**, 128–134 (2014).

[22] Green, J. K. *et al.* Large influence of soil moisture on long-term terrestrial carbon uptake. *Nature* **565**, 476479 (2019).

[23] Sack, L. *et al.* Plant hydraulics as a central hub integrating plant and ecosystem function: meeting report for 'emerging frontiers in plant hydraulics' (washington, dc, may 2015). *PLANT CELL AND ENVIRONMENT* **39**, 2085–2094 (2016).

[24] Sperry, J. S. & Love, D. M. What plant hydraulics can tell us about responses to climate-change droughts. *NEW PHYTOLOGIST* **207**, 14–27 (2015).

[25] Allen, C. D. *et al.* A global overview of drought and heat-induced tree mortality reveals emerging climate change risks for forests. *FOREST ECOLOGY AND MANAGEMENT* **259**, 660–684 (2010). Conference on Adaptation of Forests and Forest Management to Changing Climate with Emphasis on Forest Health, Umea, SWEDEN, AUG 25-28, 2008.

[26] Bonan, G. B., Williams, M., Fisher, R. A. & Oleson, K. W. Modeling stomatal conductance in the earth system: linking leaf water-use efficiency and water transport along the soil-plant-atmosphere continuum. *GEOSCIENTIFIC MODEL DEVELOPMENT* **7**, 2193–2222 (2014).

[27] Xu, X., Medvigy, D., Powers, J. S., Becknell, J. M. & Guan, K. Diversity in plant hydraulic traits explains seasonal and inter-annual variations of vegetation dynamics in seasonally dry tropical forests. *NEW PHYTOLOGIST* **212**, 80–95 (2016).

[28] Kennedy, D. *et al.* Implementing plant hydraulics in the community land model, version 5. *Journal of Advances in Modeling Earth Systems* (2019).

[29] Sperry, J. S. *et al.* Pragmatic hydraulic theory predicts stomatal responses to climatic water deficits. *NEW PHYTOLOGIST* **212**, 577–589 (2016).

[30] Amenu, G. G. & Kumar, P. A model for hydraulic redistribution incorporating coupled soil-root moisture transport. *HYDROLOGY AND EARTH SYSTEM SCIENCES* **12**, 55–74 (2008).

[31] Doussan, C., Pierret, A., Garrigues, E. & Pages, L. Water uptake by plant roots: Ii - modelling of water transfer in the soil root-system with explicit account of flow within the root system - comparison with experiments. *PLANT AND SOIL* **283**, 99–117 (2006). International Conference on Rhizosphere -Perspectives and Challenges, Munich, GERMANY, SEP, 2004.

[32] Javaux, M., Couvreur, V., Vanderborght, J. & Vereecken, H. Root water uptake: From three-dimensional biophysical processes to macroscopic modeling approaches. *VADOSE ZONE JOURNAL* **12** (2013).

[33] Couvreur, V., Vanderborght, J., Beff, L. & Javaux, M. Horizontal soil water potential heterogeneity: simplifying approaches for crop water dynamics models. *HYDROLOGY AND EARTH SYSTEM SCIENCES* **18**, 1723–1743 (2014).

[34] Lobet, G., Couvreur, V., Meunier, F., Javaux, M. & Draye, X. Plant water uptake in drying soils. *PLANT PHYSIOLOGY* **164**, 1619–1627 (2014).

[35] Sulis, M. *et al.* Incorporating a root water uptake model based on the hydraulic architecture approach in terrestrial systems simulations. *Agricultural and Forest Meteorology* **269-270**, 28 – 45 (2019).

[36] Bouda, M. & Saiers, J. E. Dynamic effects of root system architecture improve root water uptake in 1d process-based soil-root hydrodynamics. *ADVANCES IN WATER RESOURCES* **110**, 319–334 (2017).

[37] Bouda, M., Brodersen, C. & Saiers, J. Whole root system water conductance responds to both axial and radial traits and network topology over natural range of trait variation. *JOURNAL OF THEORETICAL BIOLOGY* **456**, 49–61 (2018).

[38] Landsberg, J. & Fowkes, N. Water movement through plant roots. *Annals of Botany* **42**, 493–508 (1978).

[39] Meunier, F., Draye, X., Vanderborght, J., Javaux, M. & Couvreur, V. A hybrid analytical-numerical method for solving water flow equations in root hydraulic architectures. *APPLIED MATHEMATICAL MODELLING* **52**, 648–663 (2017).

[40] Shaw, D. *et al.* Ecological setting of the wind river old-growth forest. *ECOSYSTEMS* **7**, 427–439 (2004).

[41] Warren, J., Meinzer, F., Brooks, J. & Domec, J. Vertical stratification of soil water storage and release dynamics in pacific northwest coniferous forests. *AGRICULTURAL AND FOREST METEOROLOGY* **130**, 39–58 (2005).

[42] Wharton, S. Ameriflux us-wrc wind river crane site. URL `http://dx.doi.org/10.17190/AMF/1246114`.

[43] MCBURNEY, T. & COSTIGAN, P. Measurement of stem water potential of young plants using a hygrometer attached to the stem. *JOURNAL OF EXPERIMENTAL BOTANY* **33**, 426–431 (1982).

[44] Carminati, A., Zarebanadkouki, M., Kroener, E., Ahmed, M. A. & Holz, M. Biophysical rhizosphere processes affecting root water uptake. *ANNALS OF BOTANY* **118**, 561–571 (2016).

[45] Williams, M., Bond, B. & Ryan, M. Evaluating different soil and plant hydraulic constraints on tree function using a model and sap flow data from ponderosa pine. *PLANT CELL AND ENVIRONMENT* **24**, 679–690 (2001).

[46] R.H., B. & A.T., C. Hydraulic properties of porous media. hydrology paper no. 3. Tech. Rep., Civil Engineering Department, Colorado State University. (1964).

[47] Levenberg, K. A method for the solution of certain problems in least-squares. *Quarterly Applied Mathematics* **2**, 164168 (1944).

[48] Marquardt, D. An algorithm for least-squares estimation of nonlinear parameters. *SIAM Journal Applied Mathematics* **11**, 431441 (1963).

[49] Smith, R., Smettem, K., Broadbridge, P. & Woolhiser, D. *Infiltration Theory for Hydrologic Applications*. Water Resources Monograph (Wiley, 2002). URL `https://books.google.com/books?id=MhRKAeZcxUMC`.

[50] Nocedal, J. & Wright, S. Numerical optimization. In *Springer Series in Operations Research* (Springer Verlag, New York, 2006), 2 edn.

[51] Mathworks. Matlab and statistics toolbox release 2018a (2018).